Reviews of Accelerator Science and Technology
Vol. 3 (2010) 39–56

DOI: 10.1142/S179362681000035X

World Scientific
www.worldscientific.com

Electromagnetic Radiation in Accelerator Physics

G. Stupakov
SLAC National Accelerator Laboratory, MS 26
Stanford, CA 94309, USA
stupakov@slac.stanford.edu

This article reviews some fundamental concepts and presents several recent techniques used for calculation of radiation in various environments. They include properties of longitudinal and transverse formation lengths of radiation, usage of the parabolic equation and the Kirchhoff diffraction integral in radiation, coherent radiation and fluctuations in the beam, and the radiative reaction force resulting from coherent radiation.

Keywords: Synchrotron radiation; undulator; parabolic equation; diffraction; coherent radiation; radiative reaction force.

1. Introduction

There are two broad areas of research in accelerator physics, which involve electromagnetic radiation of beams of charged particles. The first one deals mostly with the properties of the radiation itself, focusing on its intensity, angular and frequency distribution, polarization, etc. These studies are mainly motivated by various applications of the synchrotron and undulator radiation, and come predominantly from usage of relativistic beams as sources of intense radiation or usage of radiation for diagnostic purposes. The second area of research is concerned with the effect of the electromagnetic field on the beam motion, and was traditionally motivated by calculation of wake fields of the beam, and analysis of the beam instabilities caused by such wakes.

The study of radiation of charged particles in accelerators has a long history [1] goes back to the seminal papers by Schwinger [2–4], Schiff [5] and Nodvick and Saxon [6] devoted to various aspects of synchrotron radiation of relativistic particles. Interaction of beams and currents with self-fields also has deep roots in development of rf sources and microwave circuits (see e.g. [7–9]). While in the early stages of development these two fields of research did not overlap, over the last 10–15 years they have converged into a unique discipline characterized by a multitude of powerful new techniques. A good example of such convergence is given by free electron lasers, where one can trace a combination of ideas from such rf sources as klystrons and traveling wave tubes with the properties of undulator and wiggler radiation and a tight connection with the beam dynamics.

Another noticeable development of the last decade is represented by the proliferation of computer codes. These are used to numerically solve Maxwell's equations and provide invaluable results in many practically important cases, where analytical solutions are not available. In addition to solving practical problems, such codes are often used for validation of new analytical methods. They also provide an additional momentum for search of effective algorithms to solve Maxwell's equation.

In most cases radiation in accelerators can be described by classical electrodynamics, which neglects quantum effects. A well-known exception is the quantum recoil effect, which plays an important role in the beam dynamics at high energy in lepton circular machines by introducing diffusion effects into the phase space of the beam [10]. The quantum diffusion sets the scale of the beam emittance in electron and positron rings, and thus plays a crucial role in the beam dynamics. Other quantum effects in radiation involve radiative spin polarization [11] and some regimes in free electron lasers [12]. Consistent analysis of quantum effects in radiation is based on the

quantum electrodynamics and lies beyond the scope of this article.

We do not touch in this article an enormous field of numerical methods in electromagnetism. The reader interested in the latest developments of numerical methods should consult recent books and review papers (see e.g. [13–16]) on the subject.

In this article, we will try to review some fundamental concepts and present several recent techniques used for calculation of radiation in various environments. After a brief review of equations used for calculation of radiation in Secs. 2–4, we begin with a time domain analysis of synchrotron radiation in Sec. 5 and a brief introduction to the basics of undulator radiation in Sec. 6. We then discuss properties of longitudinal and transverse formation lengths of radiation, in Sec. 7. The technique of the parabolic equation is discussed in Sec. 8. In Sec. 9 we introduce the method of the Kirchhoff diffraction integral valid for short-wavelength radiation. In Secs. 10 and 11 we establish the connection between the coherent radiation and fluctuations and correlations in the beam. Finally, in Sec. 12, we discuss the radiative reaction force, also called the CSR force, resulting from coherent radiation.

2. Maxwell's Equation and Boundary Conditions

Within the classical electromagnetic theory the radiation processes are described by Maxwell's equations. In the Gaussian system of units (which we adopt in this article) Maxwell's equations in free space are [17, 18]

$$\nabla \cdot \mathbf{E} = 4\pi\rho, \tag{1a}$$

$$\nabla \cdot \mathbf{B} = 0, \tag{1b}$$

$$\nabla \times \mathbf{E} = -\frac{1}{c}\frac{\partial \mathbf{B}}{\partial t}, \tag{1c}$$

$$\nabla \times \mathbf{B} = \frac{4\pi}{c}\mathbf{j} + \frac{1}{c}\frac{\partial \mathbf{E}}{\partial t}, \tag{1d}$$

where $\mathbf{E}(\mathbf{r}, t)$ and $\mathbf{H}(\mathbf{r}, t)$ are the electric and magnetic fields, $\rho(\mathbf{r}, t)$ is the charge density, and $\mathbf{j}(\mathbf{r}, t)$ is the current density.

It is often convenient to work with Fourier components of the electric and magnetic fields. We define the Fourier transformation of function $f(t)$ as

$$\hat{f}(\omega) = \int_{-\infty}^{\infty} dt f(t) e^{i\omega t}, \tag{2}$$

and use a "hat" to indicate the Fourier image. Applying the Fourier transformation to Maxwell's equations, we find for the last two equations that involve the time variable

$$\begin{aligned} \nabla \times \hat{\mathbf{E}} &= \frac{\omega}{c}\hat{\mathbf{B}}, \\ \nabla \times \hat{\mathbf{B}} &= \frac{4\pi}{c}\hat{\mathbf{j}} - \frac{\omega}{c}\hat{\mathbf{E}}. \end{aligned} \tag{3}$$

Maxwell's equations are to be solved with appropriate initial and boundary conditions. For radiation in free space, the boundary condition is that far from the sources of radiation, $|\mathbf{r}| \to \infty$, the solution includes only waves propagating away from the sources.

In the presence of metallic boundaries, Maxwell's equations are supplemented by the boundary conditions on the surface of the metal. The two most important types of boundary conditions used in practice are the perfect conductivity approximation and the Leontovich boundary condition [19]. The former is used when one can completely neglect the resistivity of the metal, and consists in the requirement of the vanishing tangential component of the electric field, $\mathbf{E}_t = 0$, on the surface of the metal. The Leontovich boundary condition is valid in the limit when the skin depth is much smaller than the wavelength, and relates the longitudinal electric field on the surface of the metal $\hat{\mathbf{E}}_t$ (in Fourier representation) to the magnetic field,

$$\hat{\mathbf{E}}_t = \zeta \hat{\mathbf{H}} \times \mathbf{n}, \tag{4}$$

where $\mathbf{n}$ is the unit vector normal to the surface and directed toward the metal, and

$$\zeta(\omega) = \frac{1-i}{\sigma\delta(\omega)},$$

with $\delta = \sqrt{2/Z_0\sigma\omega}$ the skin depth at the given frequency, σ the metal conductivity, and $Z_0 = 4\pi/c = 377$ ohms. In the limit $\sigma \to \infty$ we have $\zeta \to 0$, and (4) reduces to the boundary condition for the perfect metal.

Maxwell's equations can be rewritten in various forms. A useful formulation, which is often employed in both analytical and numerical studies, is to eliminate the magnetic field, and obtain a second order equation for the electric field. A straightforward calculation yields

$$\nabla \times \nabla \times \mathbf{E} + \frac{1}{c^2}\frac{\partial^2 \mathbf{E}}{\partial t^2} = -\frac{4\pi}{c^2}\frac{\partial \mathbf{j}}{\partial t}. \tag{5}$$

In the absence of charges and currents, $\mathbf{j} = 0$, taking into account that the solenoidal property of the electric field in this case is $\nabla \cdot \mathbf{E} = 0$, we arrive at the well-known wave equation for the electric field in vacuum

$$\Delta \mathbf{E} + \frac{1}{c^2}\frac{\partial^2 \mathbf{E}}{\partial t^2} = 0. \tag{6}$$

3. Retarded and Liénard–Wiechert Potentials

Electromagnetic potentials $\phi(\mathbf{r}, t)$ and $\mathbf{A}(\mathbf{r}, t)$ are introduced in such a way that (1b) and (1c) are satisfied automatically. In the Lorentz gauge[a] they are related to the observable field through

$$\mathbf{E} = -\nabla\phi - \frac{1}{c}\frac{\partial \mathbf{A}}{\partial t}, \quad \mathbf{B} = \nabla \times \mathbf{A}. \tag{7}$$

Remarkably, in terms of the electromagnetic potentials Maxwell's equations in free space can be solved explicitly. This solution is often called the *retarded* potentials [18] and is given by the equations

$$\begin{aligned} \phi(\mathbf{r}, t) &= \int \frac{\rho(\mathbf{r}', t_{\text{ret}})}{|\mathbf{r} - \mathbf{r}'|} d^3 r', \\ \mathbf{A}(\mathbf{r}, t) &= \frac{1}{c}\int \frac{\mathbf{j}(\mathbf{r}', t_{\text{ret}})}{|\mathbf{r} - \mathbf{r}'|} d^3 r', \end{aligned} \tag{8}$$

where the integration is carried over the region occupied by the charges, and the retarded time $t_{\text{ret}}(\mathbf{r}, \mathbf{r}', t)$ is defined by

$$t_{\text{ret}}(\mathbf{r}, \mathbf{r}', t) = t - \frac{1}{c}|\mathbf{r} - \mathbf{r}'|. \tag{9}$$

It has a meaning of time at which the electromagnetic field that arrives at point $\mathbf{r}$ at time t has been emitted at point $\mathbf{r}'$. Substituting (8) into (7) after some transformations, one can obtain expressions for the fields in terms of the charge and current density (and their time derivatives) integrated over space; those are sometimes called Jefimenko's equations [18].

The simplicity of Eqs. (8) is deceptive: the involvement of the retarded time in the arguments of the charge density and the current makes calculations of the integrals a difficult task. However, they are often used as a starting point of calculations in various radiation problems, as well as numerical treatment of radiation problems.

Integration in (8) can be carried out for a point charge arbitrarily moving in free space along a trajectory specified by $\mathbf{r}_0(t)$. For such a charge $\rho = q\delta(\mathbf{r} - \mathbf{r}_0(t))$ and $\mathbf{j} = q\mathbf{v}(t)\delta(\mathbf{r} - \mathbf{r}_0(t))$, with $\mathbf{v} = d\mathbf{r}_0/dt$. The result is known as the Liénard–Wiechert potentials:

$$\begin{aligned} \phi(\mathbf{r}, t) &= \frac{q}{R(1 - \boldsymbol{\beta}_{\text{ret}} \cdot \mathbf{n})}, \\ \mathbf{A}(\mathbf{r}, t) &= \frac{q\boldsymbol{\beta}_{\text{ret}}}{R(1 - \boldsymbol{\beta}_{\text{ret}} \cdot \mathbf{n})}. \end{aligned} \tag{10}$$

Here the normalized particle's velocity $\boldsymbol{\beta} = \mathbf{v}/c$ should be taken at the retarded time, $\boldsymbol{\beta}_{\text{ret}} = \boldsymbol{\beta}(t_{\text{ret}})$, which is now considered as a function of $\mathbf{r}$ and t, $t_{\text{ret}}(\mathbf{r}, t)$, and is defined as a solution to the equation

$$t_{\text{ret}} = t - \frac{1}{c}|\mathbf{r} - \mathbf{r}_0(t_{\text{ret}})|. \tag{11}$$

In the above equations $\mathbf{R}(\mathbf{r}, t) = \mathbf{r} - \mathbf{r}_0(t_{\text{ret}})$ is a vector drawn from the retarded position of the particle to the observation point, $\mathbf{n}$ is a unit vector in the direction of $\mathbf{R}$, and $R = |\mathbf{R}|$.

Using (7) and (10) one can obtain formulas that express the electric and magnetic fields of an arbitrary moving point charge [see Eqs. (14.13) and (14.14) of Ref. 18]:

$$\begin{aligned} \mathbf{E} = {} & q\frac{\mathbf{n} - \boldsymbol{\beta}_{\text{ret}}}{\gamma^2 R^2 (1 - \boldsymbol{\beta}_{\text{ret}} \cdot \mathbf{n})^3} \\ & + \frac{q}{c}\frac{\mathbf{n} \times \{(\mathbf{n} - \boldsymbol{\beta}_{\text{ret}}) \times \dot{\boldsymbol{\beta}}_{\text{ret}}\}}{R(1 - \boldsymbol{\beta}_{\text{ret}} \cdot \mathbf{n})^3}, \end{aligned} \tag{12a}$$

$$\mathbf{B} = \mathbf{n} \times \mathbf{E}, \tag{12b}$$

where $\dot{\boldsymbol{\beta}}_{\text{ret}}$ is the acceleration (normalized by the speed of light) taken at the retarded time, and $\gamma = (1 - \beta^2)^{-1/2}$. These equations form a basis for calculation of the synchrotron and undulator radiation (see e.g. Refs. 21–24).

At large distance from the charge the second term of (12a), which decays as R^{-1}, dominates the first one, proportional to R^{-2}. This second term is the radiation term, while the first one is usually associated with the Coulomb field of the moving charge, sometimes also called the *velocity field*.

4. Alternative Expression for the Electromagnetic Field

To calculate the spectral and angular distributions of radiation, one has to make Fourier transformation of

[a] An illuminating discussion on gauge transformation in classical electromagnetic theory can be found in Ref. 20.

the fields (12). Using (2) and changing the integration variable from t to $t_{\rm ret}$ (which is denoted below by t') with the help of $dt = dt'(1-\mathbf{n}\cdot\boldsymbol{\beta})$, we find the Fourier image of the electric field

$$\hat{\mathbf{E}}(\mathbf{r},\omega) = \frac{e}{\gamma^2}\int_{-\infty}^{\infty} dt' \frac{\mathbf{n}-\boldsymbol{\beta}}{R^2(1-\mathbf{n}\cdot\boldsymbol{\beta})^2} e^{i\omega(t'+R/c)} + \frac{e}{c}\int_{-\infty}^{\infty} dt' \frac{\mathbf{n}\times[(\mathbf{n}-\boldsymbol{\beta})\times\dot{\boldsymbol{\beta}}]}{R(1-\mathbf{n}\cdot\boldsymbol{\beta})^2} e^{i\omega(t'+R/c)}. \tag{13}$$

Here $R, \mathbf{n}, \boldsymbol{\beta}$, and $\dot{\boldsymbol{\beta}}$ are now considered as given functions of time t'.

Recall that the usual approximation for the *far zone* (fz) is to neglect the velocity field and to take the limit $R \to \infty$:

$$\hat{\mathbf{E}}_{\rm fz}(\mathbf{r},\omega) \approx \frac{e}{cR}\int_{-\infty}^{\infty} dt' \frac{\mathbf{n}\times[(\mathbf{n}-\boldsymbol{\beta})\times\dot{\boldsymbol{\beta}}]}{(1-\mathbf{n}\cdot\boldsymbol{\beta})^2} \times e^{i\omega(t'+R/c)}.$$

In this expression, the value of R in front of the integral and the vector $\mathbf{n}$ are considered as constant but R in the exponential (and of course $\boldsymbol{\beta}$ and $\dot{\boldsymbol{\beta}}$) are functions of time. If one integrates this expression over a finite time interval from t_1 to t_2, the result is

$$\hat{\mathbf{E}}_{\rm fz}(\mathbf{r},\omega) = -\frac{ie\omega}{cR}\int_{t_1}^{t_2} dt' \mathbf{n}\times(\mathbf{n}\times\boldsymbol{\beta}) e^{i\omega(t'+R/c)} + \frac{e}{cR}\frac{\mathbf{n}\times(\mathbf{n}\times\boldsymbol{\beta})}{1-\mathbf{n}\cdot\boldsymbol{\beta}} e^{i\omega(t+R/c)}\Big|_{t_2} - \frac{e}{cR}\frac{\mathbf{n}\times(\mathbf{n}\times\boldsymbol{\beta})}{1-\mathbf{n}\cdot\boldsymbol{\beta}} e^{i\omega(t+R/c)}\Big|_{t_1}. \tag{14}$$

The last two terms are responsible for the *edge* radiation in the far zone [25].

Note that for a relativistic particle with $\gamma \gg 1$ the integrands in (13) have sharp narrow peaks at time t' when $\mathbf{n}$ is parallel to $\boldsymbol{\beta}$, because at this time the denominators $(1-\mathbf{n}\cdot\boldsymbol{\beta})^2 \sim 1/4\gamma^4$ become extremely small. This time corresponds to the moment when the particle velocity is directed toward the observation point. Because of these sharp peaks, the direct numerical computation of the field based on (13) becomes problematic for ultrarelativistic particles. There is, however, an alternative equivalent expression for the field of a moving point charge [26]:

$$\hat{\mathbf{E}}(\mathbf{r},\omega) = \frac{ie\omega}{c}\int_{-\infty}^{\infty}\frac{dt'}{R}\left[\boldsymbol{\beta}-\mathbf{n}\left(1+\frac{ic}{\omega R}\right)\right] \times e^{i\omega(t'+R/c)}. \tag{15}$$

Although this equation looks very different from (and much simpler than) (13), it gives the same result for $\hat{\mathbf{E}}(\mathbf{r},\omega)$. The derivation of (15) using Liénard–Wiechert potentials is given in the Appendix. This equation forms the basis for numerical algorithm of the Synchrotron Radiation Workshop computer code [27].

5. Time Domain versus Frequency Domain in Synchrotron Radiation

Traditionally, synchrotron radiation is analyzed in the frequency domain [18, 21–24]. In an alternative and complementary approach one can look at the time structure of radiation pulses [28], which gives a new insight into this classical radiation problem. In particular, using the time domain approach helps one to understand some properties of radiation from short magnets.

Consider a point charge moving with relativistic velocity ($\gamma \gg 1$) in a circular orbit of radius ρ, as shown in Fig. 1. The position of the particle is determined by angle φ, with $\varphi = 0$ corresponding to the origin of the coordinate system. An observer is located at point O in the plane of the orbit, at distance r from the origin, far from the particle. The observer will see a periodic sequence of pulses of electromagnetic radiation with the period equal to the revolution period T_0. Each pulse is emitted from a

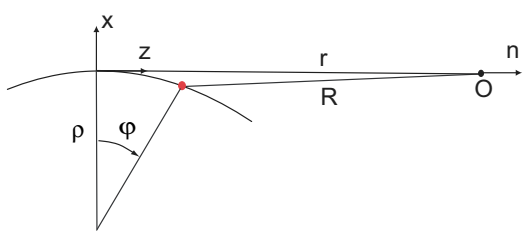

Fig. 1. A schematic showing a part of a cicular orbit and the observation point O. The position of the particle is shown by the red dot. The Cartesian coordinate system is chosen in such a way that its origin is located on the orbit and the z axis is tangential to the circle and directed toward O. The y axis is directed out of the page.

small fraction of the orbit, $x, z \ll \rho$. We denote the electric field of the pulse at the observation point by $E(t)$.

If we synchronize the clock in such a way that at $t = 0$ the particle is passing through the origin of the coordinate system, then the position of the particle at time t is characterized by the angle $\varphi = \omega_0 t$, with $\omega_0 = 2\pi/T_0$ the angular revolution frequency of the particle. The electromagnetic pulse arrives at point O at time $t \approx r/c$. It is convenient to introduce the dimensionless time variable $\tilde{t} = (\gamma^3 c/\rho)(t - r/c)$ and the dimensionless electric field $\tilde{E} = (r\rho/4q\gamma^4)E_x$. Using Taylor expansion of the field at the observation point around $\tilde{t} = 0$, one can show that the dependence $\tilde{E}(\tilde{t})$ is given by the implicit relations [29]

$$\tilde{E} = \frac{1-\zeta^2}{(\zeta^2+1)^3}, \quad \tilde{t} = \frac{1}{2}\zeta + \frac{1}{6}\zeta^3, \tag{16}$$

where the variable ζ is related to the position on the circle through $\zeta = \varphi\gamma$. These equations associate each point on the curve $\tilde{E}(\tilde{t})$ with a position on the circle and the corresponding moment of emission, and hence connect the radiation properties to the geometry of the orbit. The plot of the function $\tilde{E}(\tilde{t})$ is shown in Fig. 2; it is an even function of $\tilde{t}$. We see from this plot that the characteristic width of the pulse $\Delta\tilde{t} \sim 1$, which means that the duration of the pulse in physical units is

$$\Delta t \sim \frac{\rho}{c\gamma^3}. \tag{17}$$

This corresponds to the width of the radiation spectrum $\Delta\omega \sim c\gamma^3/\rho$, in agreement with the fact that the main energy of the synchrotron radiation is localized in the frequency range of the order of the critical frequency $\omega_c = c\gamma^3/\rho$ [18].

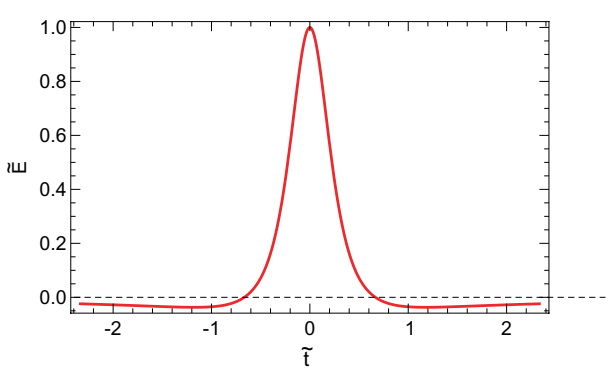

Fig. 2. The radiation pulse of the electromagnetic field in dimensionless variables.

The pulse in Fig. 2 has a positive core and long negative tails where, for $|\tilde{t}| \gg 1$, we have $\tilde{E} \approx -1/(6|\tilde{t}|)^{4/3}$. The long tails determine the low-frequency part of the spectrum of the radiation with $\omega \ll \omega_c$.

A straighforward integration shows that the area under the curve in Fig. 2 is equal to zero:

$$\int_{-\infty}^{\infty} dt E = 0. \tag{18}$$

This is not accidental — it is a demonstration of the general principle applicable to any radiating system of finite size [30]. It is equivalent to the statement that such systems do not radiate at zero frequency, which is rather evident, because the zero-frequency field is static and cannot propagate away from the source.

As was mentioned at the beginning of this section, the time domain analysis allows one to easily explain several features of synchrotron radiation from a short magnet [31], when a point charge is moving on an arc of a circle. Let us assume that the angular extension of the arc is $\varphi_{\min} < \varphi < \varphi_{\max}$, and outside of the arc the particle is moving along straight lines (tangential to the end points of the arc) with constant velocity. Since there is no acceleration on the straight parts of the orbit, the radiation pulse shown in Fig. 2 will be truncated: the value of the radiation field $\tilde{E}$ becomes zero for $\varphi < \varphi_{\min}$ and $\varphi_{\max} < \varphi$, while it remains the same for the points on the arc where $\varphi_{\min} < \varphi < \varphi_{\max}$. Remembering the relation $\zeta = \gamma\varphi$, we conclude that the radiation pulse for a short magnet is given by the same equations, (16), where ζ is now constrained by $\varphi_{\min}/\gamma < \zeta < \varphi_{\max}/\gamma$. An example of the pulse shape for $\varphi_{\min}/\gamma = -0.5$ and $\varphi_{\max}/\gamma = 0.7$ is shown in Fig. 3. The discontinuities of the field at the front and the tail of the pulse generate so-called edge radiation,[b] [25, 32] represented by last two terms of (14).

It is interesting to note that for the pulse in Fig. 3 Eq. (18) does not hold. This is due to the fact that the complete trajectory of the charge (with incoming and outgoing straight lines) is not confined

[b] In reality, the abrupt changes of the field will be somewhat smeared out due to finite extension of the edge magnetic field at the entrance to and the exit from the magnet.

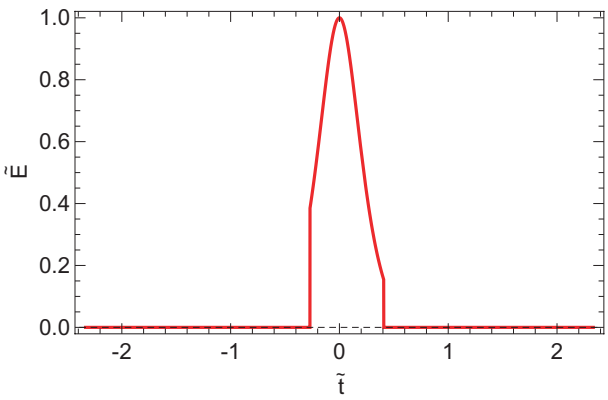

Fig. 3. The radiation pulse of the electromagnetic field for a short magnet with $\varphi_{\min}/\gamma = -0.5$ and $\varphi_{\max}/\gamma = 0.7$.

to a limited region of space (in contrast to a circular trajectory) but infinitely extends in both directions in z. A charge moving on such an unconstrained orbit creates a static field that decays inversely proportional to the distance from the orbit. This results in a nonvanishing zero harmonic of the field, $\hat{\mathbf{E}}|_{\omega=0} \neq 0$. One of the consequences of nonzero $\hat{\mathbf{E}}|_{\omega=0}$ is that the spectrum of the pulse shown in Fig. 3 is much richer in low frequencies than the one shown in Fig. 2 [33]. A more detailed analysis of violation of the condition (18) in the case of an arc is given in Ref. 28.

6. Basics of Undulator Radiation

An undulator is a spatially periodic magnetic structure used for generation of quasi-monochromatic radiation. There are several ways to derive the undulator radiation. The most direct approach is to analyze the electromagnetic field with the Liénard–Wiechert equations (12) in the far zone of a point charge passing through an undulator. Alternatively, one can connect the undulator radiation with another well-known phenomenon in electromagnetic theory — the Thomson scattering. We will demonstrate the latter in what follows.

Let us consider a plane undulator with the magnetic field given by

$$B_y(z) = B_0 \cos k_u z, \tag{19}$$

with the undulator period $\lambda_u = 2\pi/k_u$. The undulator is characterized by the amplitude magnetic field B_0, the period λ_u, and the number of periods N_u. We assume that a relativistic particle propagates along the z axis with velocity v close to the speed of light.

Let us now consider the process of radiation in the particle's frame of reference. To find the undulator field in this frame, we note that relative to the particle the undulator is moving in the negative direction of the z axis with velocity $\mathbf{v} = (0, 0, -v)$. Using the Lorentz transformation for coordinates and time, we find that

$$z = \gamma(z' - \beta ct') \approx \gamma(z' - ct'), \tag{20}$$

where we mark by a prime all quantities in the particle's frame. Assuming that $\gamma \gg 1$ and using the Lorentz transformation for the fields, we can also find the undulator field in the particle's frame:

$$\begin{aligned} E'_x &= \gamma\beta B_0 \cos k_u z \approx \gamma B_0 \cos k_u \gamma(z' - ct'), \\ B'_y &= \gamma B_0 \cos k_u z \approx \gamma B_0 \cos k_u \gamma(z' - ct'). \end{aligned} \tag{21}$$

First, we see that in addition to the magnetic there is an electric field in the x direction, perpendicular to the direction of motion and the magnetic field. Moreover, the magnitude of the electric field is equal to that of the magnetic one, and both are γ times larger than the lab field of the undulator. To a good approximation, the electromagnetic field is indistinguishable from a plane electromagnetic wave with the frequency $\omega' = \gamma k_u c$ moving in the negative z direction. Under the influence of this field the electron starts to oscillate and radiate secondary waves, and this is exactly the problem of the Thomson scattering.

Before we proceed further, we have to estimate the velocity of the oscillations and compare it with the speed of light. Consider a particle located at $z' = 0$. Inside the electromagnetic field its velocity is $v_x = v_{\text{osc}} \cos \omega' t'$, where v_{osc} is the amplitude of the oscillating velocity. Assuming that $v_{\text{osc}} \ll c$, it is easy to find $v_{\text{osc}} = eE'_x/m\omega' = eB_0/mk_u c$. This introduces the *undulator parameter* K, equal to v_{osc}/c:

$$K = \frac{eB_0}{k_u mc}. \tag{22}$$

In what follows, we will require $K \ll 1$; in this limit the frequency of the scattered wave is equal to the frequency ω' of the incident one.

The intensity of the Thomson-scattered radiation can be found in textbooks [18]: it is proportional to the square of the amplitude of the electric field, which in our case is equal to γB_0:

$$\frac{d\mathcal{I}'}{d\Omega'} = \frac{e^4\gamma^2 B_0^2}{8\pi c^3 m^2}(1 - \sin^2\theta' \cos^2\phi'), \tag{23}$$

where $d\mathcal{I}'/d\Omega'$ is the the intensity of the radiation per unit solid angle in the direction characterized by the polar angle θ' and the azimuthal angle ϕ' (in the spherical coordinate system with the z axis along the direction of propagation of the wave). We now need to transform the quantities $d\mathcal{I}'$, $d\Omega'$, θ', and ω' into the lab frame (the angles ψ and ψ' are equal). The Lorentz transformation for the angles gives

$$\sin\theta' = \frac{\sin\theta}{\gamma(1-\beta\cos\theta)} \approx \frac{2\theta\gamma}{1+\gamma^2\theta^2}, \qquad (24)$$

where we have assumed that $\theta \ll 1$, expanded $\cos\theta \approx 1-\theta^2/2$, and used $1-\beta \approx 1/2\gamma^2$. From the Lorentz transformation for frequencies we also find that

$$\omega \approx \frac{2\gamma\omega'}{1+\gamma^2\theta^2} = \frac{2\gamma^2 k_u c}{1+\gamma^2\theta^2}. \qquad (25)$$

This equation associates with each angle θ the frequency of the radiation that propagates in that direction. The maximum frequency in the lab frame goes in the forward direction, $\theta = 0$, and is equal to

$$\omega_0 = 2\gamma\omega' = 2\gamma^2 k_u c. \qquad (26)$$

The differential of the solid angle is transformed like

$$d\Omega' = \sin(\theta')d\theta' d\phi' = |d\cos(\theta')|d\phi, \qquad (27)$$

from which we find that

$$d\Omega' = \frac{1-\beta^2}{(1-\beta\cos\theta)^2}|d\cos(\theta)|d\phi \approx \frac{4\gamma^2}{(1+\gamma^2\theta^2)^2}d\Omega. \qquad (28)$$

Finally, we need to transform the differential $d\mathcal{I}'$, which is the radiated energy of the electromagnetic field per unit time: $d\mathcal{I}' = dE'/dt'$. The Lorentz transformation of time is $dt' = dt/\gamma$. The easiest way to transform the energy is to invoke the quantum theory and to consider radiation as a collection of photons. In quantum language the energy of a photon is $\hbar\omega$, and the number of photons $N_{\rm ph}$ is the same in any reference frame. Hence the energy is transformed as the frequency, and $dE' = N_{\rm ph}\hbar\omega' = dE(\omega'/\omega)$. This allows us to convert $d\mathcal{I}'/d\Omega'$ into the beam frame:

$$\frac{d\mathcal{I}}{d\Omega} = \frac{dE}{d\Omega dt} = \frac{dE'}{d\Omega' dt'}\frac{\omega}{\omega'}\frac{1}{\gamma}\frac{4\gamma^2}{(1+\gamma^2\theta^2)^2} = \frac{e^4\gamma^4 B_0^2}{\pi c m^2}\frac{(1+\gamma^2\theta^2)^2 - 4\theta^2\gamma^2\cos^2\phi}{(1+\gamma^2\theta^2)^5}. \qquad (29)$$

To find the energy radiated per unit time in all angles, we integrate this equation over the solid angle using the approximation $d\Omega = d\phi\sin(\theta)d\theta \approx d\phi\theta d\theta$:

$$\mathcal{I}_0 = \int\frac{d\mathcal{I}}{d\Omega}d\Omega \approx \int_0^\infty \theta d\theta\int_0^{2\pi} d\phi\frac{d\mathcal{I}}{d\Omega} = \frac{e^4\gamma^2 B_0^2}{3cm^2}. \qquad (30)$$

Note that the radiated power from the undulator, per unit time, is equal to the radiated power from a bending magnet with the same averaged magnetic field.

Since the angle θ is uniquely associated with the frequency via (25), Eq. (29) also determines the spectrum of the undulator radiation. To find this spectrum of radiation, we need to integrate Eq. (29) over ϕ and in the final result express θ through ω using (25). This can be done analytically and leads to the following expression for the intensity of the radiation per unit frequency,

$$\frac{d\mathcal{I}}{d\omega} = \frac{3\mathcal{I}_0}{\omega_0}\frac{\omega}{\omega_0}\left(2\left(\frac{\omega}{\omega_0}\right)^2 - 2\left(\frac{\omega}{\omega_0}\right) + 1\right), \qquad (31)$$

for $\omega < \omega_0$ and zero for $\omega > \omega_0$. The plot of this function is shown in Fig. 4.

To find the radiated energy, rather than the power, one has to multiply Eqs. (29)–(31) by the time of flight through the undulator $N_u\lambda_u/c$.

In our analysis above we implicitly assumed an infinite duration of the Thomson scattering process, which, strictly speaking, corresponds to the limit $N_u \to \infty$. This has led us to the one-to-one correspondence (25) between the angle and the frequency. A more accurate analysis that takes into account

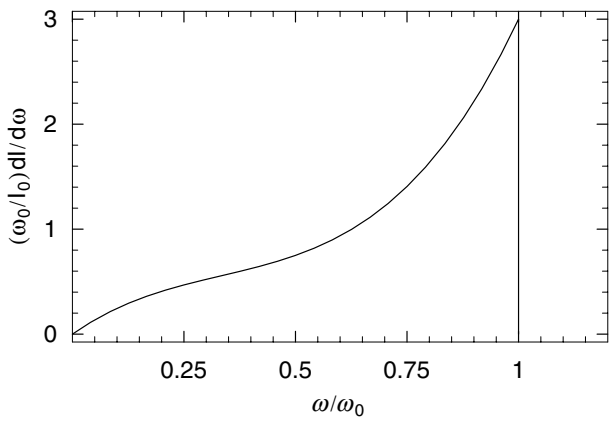

Fig. 4. The spectrum of the undulator radiation given by Eq. (31).

finite, though large, N_u shows that there is a frequency spread, $\Delta\omega \sim \omega/N_u$, in the spectral content of the radiation propagating at a given θ.

In principle, the radiation for an undulator with large K can be obtained analogously to the case $K \ll 1$. However, the calculations are much more combersome, because the particle's motion in the beam frame becomes relativistic. The interested reader can find a detailed analysis of the undulator radiation in Refs. 21–24.

7. Longitudinal and Transverse Formation Lengths

It takes some time and space around the orbit for a moving charge to generate radiation. This is a fundamental fact which is not always emphasized in calculations of various radiation processes. Evaluation of spatial scales involved in formation of radiation is an important element of understanding whether analytical results derived for free space are applicable to practical problems. In accelerators a particle's orbit is surrounded by material walls, and if they are located inside the formation volume, radiation will be strongly affected by the presence of the walls. In such a case, free space results become invalid, and one has to solve the problem taking account of the material boundaries in the system.

One comment is necessary before we proceed. The formation length is not an exact quantity which is rigorously defined by a mathematical formula. While it can always be estimated by order of magnitude, one cannot specify it with an accuracy better than a factor of order of 1. Even with this uncertainty, however, the notion of the formation length turns out to be extremely useful in applications.

To illustrate the concept of the formation length, we again consider the synchrotron radiation and use the results of the previous section. The width of the electromagnetic pulse in Fig. 2, $\Delta\tilde{t} \sim 1$, means that $\Delta\zeta \sim 1$, and through the relation $\zeta = \gamma\varphi$ translates into the angular length of the trajectory which contributes to the main body of the pulse, $\Delta\varphi \sim 1/\gamma$. Hence the length of the orbit necessary for formation of the radiation pulse, which we call the *longitudinal formation length*, $l_\parallel$, is

$$l_\parallel \sim \frac{\rho}{\gamma}. \tag{32}$$

As an immediate consequence of this equation, we conclude that if a bending magnet has a length smaller than ρ/γ, the radiation pulse gets truncated (see Fig. 3), and the spectrum of radiation changes from the one calculated for a circular orbit.

Note that using the angular spread of the synchrotron radiation $\Delta\theta \sim 1/\gamma$ and the reduced wavelength $\lambda\!\!\!^{-} = \lambda/2\pi \sim \rho/\gamma^3$, one can also write the longitudinal formation length as

$$l_\parallel \sim \frac{\lambda\!\!\!^{-}}{\Delta\theta^2}. \tag{33}$$

This equation can be better understood if one calculates the distance on which a relativistic particle ($v \approx c$) slips in phase of the order of π with a plane electromagnetic wave propagating at angle $\Delta\theta$ to the direction of motion of the particle. Since the phase velocity of the wave in the direction of motion of the particle is $c/\cos\Delta\theta$, the slippage length is estimated as $\lambda\!\!\!^{-}/(1-\cos^{-1}\Delta\theta) \sim \lambda\!\!\!^{-}/\Delta\theta^2$, in agreement with (33).

The notion of the formation length is much more general and fundamental than implied by our derivation. It is introduced in the quantum theory of radiation [34] (where it is often called the *coherence length*, [35]) as a length associated with the momentum transfer q to the external field by the radiating particle. The longitudinal formation length is related to the momentum transfer in the direction of motion: $l_\parallel \sim \hbar/q_\parallel$.

A more subtle but practically important question is: How to define the formation length for low frequencies, $\omega \ll \omega_c$? To answer this question, observe that, as follows from the uncertainty principle, formation of frequency ω involves the time interval $T \sim 1/\omega$. For $\omega \ll \omega_c$, the dimensionless time $\tilde{t}$ associated with T is $\tilde{t} = (\gamma^3 c/\rho)T \sim \gamma^3 c/\rho\omega \gg 1$. This large T includes the long tails of the radiation pulse, where, as follows from the second of Eqs. (16), $\zeta \approx (6\tilde{t})^{1/3}$. Using again the relation $\zeta = \gamma\varphi$, we arrive at the following result: the length of the orbit (in angular units) required to generate harmonic ω is $\Delta\varphi \sim (c/\rho\omega)^{1/3}$. We can also write it in terms of the *frequency-dependent* formation length $l_\parallel(\omega)$:

$$l_\parallel(\omega) \sim \rho\Delta\varphi \sim \rho^{2/3}\lambda\!\!\!^{-1/3}, \tag{34}$$

where $\lambda\!\!\!^{-} = c/\omega$. For the critical frequency $\omega = \omega_c$ this formula gives us the previous expression, (32).

Note that (34) can also be obtained from Eq. (33) taking into account that the angular spread of radiation at small frequencies $\Delta\theta \sim (\lambda\!\!\!^{-}/\rho)^{1/3}$.

The practical importance of the formation length is that to generate the full spectrum of the synchrotron radiation the length of the bending magnet should be several times longer than $l_{\parallel}(\omega)$. Radiation from a magnet that is shorter than $l_{\parallel}(\omega)$ will have properties different from that for a circular motion.

In addition to having a necessary path length, the charge needs some space in the direction perpendicular to the orbit to form radiation. We can evaluate this length, which we will call the *transverse coherence length*, $l_{\perp}$, using the following arguments. If the characteristic angular spread of the radiation is $\Delta\theta$ and the wave number is $k = \omega/c$, the transverse component of the wave number is $k_{\perp} = k\Delta\theta$. From the Fourier uncertainty principle, the transverse dimension needed to accommodate the transverse wave number is $l_{\perp} \sim 1/k_{\perp} \sim \lambda\!\!\!^{-}/\Delta\theta$. We can now use the known angular spread of the synchrotron radiation as a function of frequency, $\Delta\theta \sim (\lambda\!\!\!^{-}/\rho)^{1/3}$, to obtain

$$l_{\perp}(\omega) \sim \frac{\lambda\!\!\!^{-}}{\Delta\theta} \sim \rho^{1/3}\lambda\!\!\!^{-2/3}. \tag{35}$$

The length $l_{\perp}$ is also associated with the transverse source size for the synchrotron radiation — it is equal to the size of the image to which the particle's radiation can be focused with 1:1 optics [21].

One of the practical consequences of the transverse formation length is that the radiation can be suppressed by metal walls, if they are put close to the beam. More specifically, if the beam propagates through a dipole magnet in a metal pipe with a transverse size a, the radiation with $l_{\perp}(\omega) \gtrsim a$ or $\lambda\!\!\!^{-} \gtrsim \sqrt{a^3/\rho}$ is suppressed. This is called a *shielding* effect of the metallic pipe [2, 3, 36, 37]. It plays an important role in the modern accelerator, by limiting the energy loss of the beam on coherent radiation.

8. Parabolic Equation in Electromagnetic Problems

The *parabolic equation* (PE) in diffraction theory was proposed many years ago [38] and has been widely used since that time for solution of various electrodynamic problems. It is applicable to situations where the electromagnetic field can be considered as a monochromatic wave with a slowly-varying-in-space amplitude. This usually means that the field is composed of harmonics that propagate at small angles to the axis of the system — a property that is described by a *paraxial*, or small-angle, approximation. The PE is routinely used for studies of propagation of laser beams (such as analysis of Hermite–Gaussian and Laguerre–Gaussian modes in wave optics [39]). It is also a part of the standard approximation in a three-dimensional theory of free electron lasers [40].

To derive the PE, we denote by $\bar{\mathbf{E}}$ the Fourier-transformed electric field multiplied by the factor e^{-ikz},

$$\bar{\mathbf{E}} = e^{-ikz}\hat{\mathbf{E}}, \tag{36}$$

with $k = \omega/c$. Here we assume that the field propagates in the z direction. We then use the Fourier-transformed Eq. (5), which, with the help of $\nabla\cdot\hat{\mathbf{E}} = 4\pi\hat{\rho}$, can be written as

$$4\pi\nabla\hat{\rho} - \nabla^2\hat{\mathbf{E}} - \frac{\omega^2}{c^2}\hat{\mathbf{E}} = i\omega\frac{4\pi}{c^2}\hat{\mathbf{j}}. \tag{37}$$

We now assume that the current is directed along the z axis, so that its perpendicular components can be neglected; $\hat{\mathbf{j}}_{\perp} = 0$. Taking the transverse part of (37), we then obtain

$$\nabla^2\hat{\mathbf{E}}_{\perp} + \frac{\omega^2}{c^2}\hat{\mathbf{E}}_{\perp} = 4\pi\nabla_{\perp}\hat{\rho}, \tag{38}$$

where $\hat{\mathbf{E}}_{\perp}$ is a two-dimensional vector $\hat{\mathbf{E}}_{\perp} = (\hat{E}_x, \hat{E}_y)$ and $\nabla_{\perp} = (\partial/\partial x, \partial/\partial y)$. We now substitute $\hat{\mathbf{E}} = e^{ikz}\bar{\mathbf{E}}$ and $\hat{\rho} = e^{ikz}\bar{\rho}$ into this equation:

$$\frac{\partial^2\bar{\mathbf{E}}_{\perp}}{\partial z^2} + 2ik\frac{\partial\bar{\mathbf{E}}_{\perp}}{\partial z} + \nabla_{\perp}^2\bar{\mathbf{E}}_{\perp} = 4\pi\nabla_{\perp}\bar{\rho}. \tag{39}$$

We neglect the second derivative $\partial^2\bar{\mathbf{E}}_{\perp}/\partial z^2$ in comparison with $k\partial\bar{\mathbf{E}}_{\perp}/\partial z$, which is justified if variation of the electric field amplitude $\bar{\mathbf{E}}$ along the z axis is relatively small on the wavelength $2\pi/k$. This leads us to the PE

$$\frac{\partial\bar{\mathbf{E}}_{\perp}}{\partial z} = \frac{i}{2k}(\nabla_{\perp}^2\bar{\mathbf{E}}_{\perp} - 4\pi\nabla_{\perp}\bar{\rho}). \tag{40}$$

For a known charge distribution, it describes evolution of the transverse components of the field along the z axis. The longitudinal component can be expressed through the transverse one and the charge density using again $\nabla\cdot\hat{\mathbf{E}} = 4\pi\hat{\rho}$ written in terms of the bar quantities

$$\frac{\partial\bar{E}_z}{\partial z} + ik\bar{E}_z + \nabla_{\perp}\bar{\mathbf{E}}_{\perp} = 4\pi\bar{\rho}. \tag{41}$$

Again, neglecting the first term on the left hand side, $\partial\bar{E}_z/\partial z$, in comparison with $ik\bar{E}_z$, and expressing $\bar{E}_z$ through the transverse field yields

$$\bar{E}_z = \frac{i}{k}(\nabla_\perp \bar{\mathbf{E}}_\perp - 4\pi\bar{\rho}). \tag{42}$$

Equations (40) and (42), complemented with appropriate boundary conditions, define all components of the electric field in the system.

One of the most important advantages of the PE is that it eliminates the small wavelength $\lambda\!\!\!^{-}$ from the problem. Indeed, a simple scaling analysis of (40) shows that the longitudinal scale l of variation of the field in the z direction is of the order of $l \sim a^2/\lambda\!\!\!^{-}$, where a is the transverse size of the region occupied by the field. If $a \gg \lambda\!\!\!^{-}$, then also $l \gg a \gg \lambda\!\!\!^{-}$. As a result, numerical solution of the PE requires only a coarse spatial mesh with the mesh size that can be much larger than $\lambda\!\!\!^{-}$.

There are many electromagnetic problems in accelerator physics to which the PE can be applied. This is explained by the fact that radiation of relativistic beams at high frequencies propagates at small angles to the direction of motion, and hence is paraxial in its origin. This was clearly demonstrated in Ref. 41, where the authors used the parabolic Green function to reproduce many known results for synchrotron, transition, and undulator radiation in vacuum.

One of the areas where the PE turned out to be extremely useful is calculation of wakefields and impedances for various elements of the accelerator vacuum chamber in the high-frequency limit [42, 43] — the problem motivated by the small bunch length of electron beams in modern accelerators. In the presence of material boundaries, if transverse apertures in the system are noticeably larger than the wavelength of interest, they do not destroy the paraxial propagation of the emitted field. Direct numerical computation of wakefields based on solution of Maxwell's equations for such beams requires extremely fine meshes and demands excessive processing power from computers. It is interesting to note that although the PE neglects the backward-propagating waves reflected from obstacles in the chamber and incorrectly treats the waves propagating at large angles to the axis, nonetheless the impedance calculations are accurate because those waves do not catch up with the beam and hence do not contribute to the impedance.

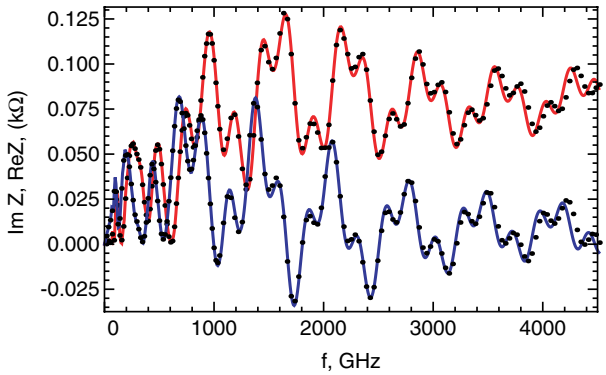

Fig. 5. Real (red) and imaginary (blue) parts of the impedance. Dots are calculated with the PE, solid lines are the result of the computer code ECHO.

As an illustration, we show in Fig. 5 the longitudinal impedance of a round tapered collimator calculated with the PE up to a frequency of about 4 THz. The collimator has two tapered transitions of length 30 mm from a radius of 5 mm to a radius of 2.5 mm. It has also a central part (2.5 mm radius) of length 30 mm. The result is compared with simulation with the computer code ECHO [44], and shows excellent agreement.

The PE was derived above for a system where the beam propagates along a straight line (the z axis). With minor modifications, it can also be applied to a circular orbit, with a beam propagating inside a vacuum chamber with conducting metallic walls. This approach was first developed in Refs. 45 and 46 for a rectangular toroidal pipe and applied to the problem of coherent synchrotron radiation. More recently it was generalized for a combination of toroidal and straight pipes [47, 48], allowing one to study synchrotron radiation inside a vacuum chamber in several dipole magnets connected by straight sections.

9. Diffraction Radiation and Kirchhoff Integral

In the presence of material boundaries one has to solve Maxwell's equations with appropriate boundary conditions, as discussed in Sec. 2. Typically, such problems are much more complicated than radiation in free space, and often cannot be solved analytically. There is, however, an important limit amenable to analytical methods, when the wavelengths of interest are small compared to the size of the apertures

in the problem. In this case one can use an approximate formulation based on the vectorial version of the diffraction theory [18]. It is interesting to note that this integral can be derived from the PE discussed in Sec. 8 by solving an initial value problem with Green's function.

Traditionally, the diffraction theory considers scattering of an electromagnetic wave emitted by a remote source on a given aperture. In the accelerator physics context, however, there are situations where the radiation source is a beam that passes through the same aperture — the radiation in this case is called the *diffraction radiation*. With a slight modification of the classical Kirchhoff integral, these problems can also be solved in the diffraction approximation [34]. We will illustrate below the technique in a particular example of radiation of a relativistic charge particle passing through a circular aperture in a conducting plane screen shown in Fig. 6, following the analysis of Ref. 34. Due to the relative simplicity of the problem, it also allows for a rigorous mathematical formulation in terms of coupled singular integral equations which can be solved numerically [49]. The simplified approach presented below has, however, the considerable advantages of simplicity and transparency.

We consider a relativistic point charge, $\gamma \gg 1$, moving along the z axis with velocity v. The origin of the coordinate system is located at the center of the hole. As already mentioned, our approach is valid if the reduced wavelength of the radiation $\lambda\!\!\!^{-} = \lambda/2\pi$ is much smaller than the radius of the hole a. As it turns out, under this condition most of the radiation propagates at small angles to the direction of motion of the charge, $\theta \ll 1$. According to the vectorial formulation of the diffraction theory, in Ref. 18 (Sec. 10.7), the field behind the screen, $\boldsymbol{\mathcal{E}}$, at large distance $R \to \infty$ in the region $z > 0$, can be

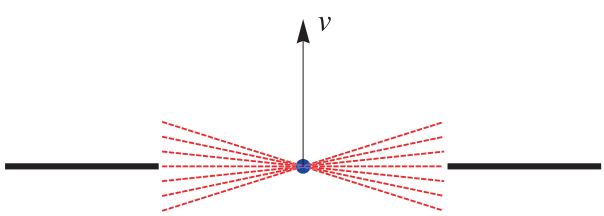

Fig. 6. A relativistic charge (shown by the blue dot) moving with velocity v is passing through a round hole in a conducting screen (shown by the black thick lines). The red dashed lines indicate electric field lines being truncated by the screen.

calculated by integrating the incident field $\boldsymbol{\mathcal{E}}_0$ on the screen at $z = 0$:

$$\boldsymbol{\mathcal{E}} = \frac{e^{ikR}}{R}\frac{i}{2\pi}\mathbf{k} \times \int_{\text{hole}} e^{-i\mathbf{kr}}\mathbf{n} \times \boldsymbol{\mathcal{E}}_0 dS, \qquad (43)$$

where $\mathbf{r} = (x, y)$ is the two-dimensional vector in the plane of the hole, $\mathbf{k}$ is the wave number vector in the direction of the radiation, $k = |\mathbf{k}| = \omega/c$, and $\mathbf{n}$ is the unit vector perpendicular to the surface of the hole. The integration in Eq. (43) goes over the cross section of the hole.

Equation (43) is derived in Ref. 18 for the case where the incident wave propagates in free space. In our problem the incident field is the Coulomb field carried by the particle. In this case, Eq. (43) gives the total field behind the screen, including the field of the particle, and to find the radiation field, $\boldsymbol{\mathcal{E}}_1$, we need to subtract the Coulomb field of the electron $\boldsymbol{\mathcal{E}}_{\text{C}}$. The latter can be calculated as the same integral in Eq. (43) in the limit $a \to \infty$, i.e. when the screen is removed. The result of such a subtraction is an integral, with the sign opposite to that in Eq. (43), in which the integration goes over the screen surface, rather than the hole [34]:

$$\begin{aligned}\boldsymbol{\mathcal{E}}_1 &= \boldsymbol{\mathcal{E}} - \boldsymbol{\mathcal{E}}_{\text{C}} \\ &= -\frac{e^{ikR}}{R}\frac{i}{2\pi}\mathbf{k} \times \int_{\text{screen}} e^{-i\mathbf{kr}}\mathbf{n} \times \boldsymbol{\mathcal{E}}_0 dS. \end{aligned} \qquad (44)$$

A more rigorous proof of this equation can be found in Ref. 50.

In the limit of a large Lorentz factor, $\gamma \gg 1$, the radial electric and azimuthal magnetic fields of the particle are

$$E_{r0} = H_{\theta 0} = \frac{e\gamma r}{[r^2 + \gamma^2(z - vt)^2]^{3/2}}, \qquad (45)$$

where $r = \sqrt{x^2 + y^2}$ is the distance from the orbit. The particle's field on the screen is given by $E_{r0}(r, 0, t)$ and $H_{\theta 0}(r, 0, t)$ in Eq. (45). Fourier transformation of these fields defined by Eq. (2) gives

$$\mathcal{E}_{r0}(r, \omega) = \mathcal{H}_{\theta 0}(r, \omega) \approx \frac{ke}{\pi c\gamma} K_1\left(\frac{kr}{\gamma}\right), \qquad (46)$$

where K_1 is the modified Bessel function of the first order, and we have used $v \approx c$ in the above expression.

In the limit of large γ, the angle of the radiation relative to the z axis, θ, is small: $\theta \ll 1$. Substituting (46) into (44) and neglecting higher-order terms in

θ, we find that $\mathcal{E}_1$ has the radial component only:

$$\mathcal{E}_{r1} = -k\frac{e^{ikR}}{R}\int_a^\infty rdr\mathcal{E}_{r0}(r,\omega)J_1(kr\theta)$$
$$= -\frac{ek^2}{\pi\gamma c}\frac{e^{ikR}}{R}\int_a^\infty rdrK_1\left(\frac{kr}{\gamma}\right)J_1(kr\theta), \quad (47)$$

where J_1 is the Bessel function of the first order. The integration in the last formula can be carried out analytically [51]:

$$\mathcal{E}_{r1} = A(\omega,\theta)\frac{e^{ikR}}{R}, \quad (48)$$

with

$$A(\omega,\theta) = \frac{e}{\pi\gamma c}\frac{ka}{\theta^2+\gamma^{-2}}\left[\theta J_2(ka\theta)K_1\left(\frac{ka}{\gamma}\right)\right.$$
$$\left. - \frac{1}{\gamma}J_1(ka\theta)K_2\left(\frac{ka}{\gamma}\right)\right]. \quad (49)$$

The quantity $|A|^2$ gives the angular and spectral distribution of the radiation. This formula agrees with the rigorous solution to the diffraction radiation problem obtained in Ref. 49, if one takes the limit $\gamma \gg 1, ka \gg 1$ of their result. In the limit $\lambda\!\!\!^{-} \gg a\gamma^{-1}$ (but with $\lambda\!\!\!^{-}$ still much less than a) we have [34]

$$A(\omega,\theta) = -\frac{e}{\pi c}\frac{\theta}{\theta^2+\gamma^{-2}}J_0(ka\theta), \quad (50)$$

which in a small-angle approximation yields

$$A(\omega,\theta) = -\frac{e}{\pi c}\frac{\theta}{\theta^2+\gamma^{-2}}. \quad (51)$$

Since the hole radius a drops out from the last equation, it is also valid in the limit $a \to 0$, when there is no hole in the screen. In this limit, it is usually called the *transition radiation*.

The reader can find further development of the method and some of its applications in Refs. 52–57.

10. Coherent Radiation and Fluctuations

Radiation of a beam is to be computed taking account of interference of electromagnetic fields emitted by different particles. This leads to the notions of *incoherent* and *coherent* components of the radiated field. The energy of the incoherent part scales linearly with the number N of particles in the beam, while the coherent radiation is proportional to N^2. In addition to these well-known characteristics of the radiation of an ensemble of particles, another important characteristic of beam radiation is its *fluctuations* caused by randomness of particle positions in the bunch. The fluctuations carry important information about distribution of particles in the beam, and can be used, for example, for diagnostic purposes [58–60].

Let us consider a one-dimensional model of the beam and assume that each particle radiates an electromagnetic pulse with the electric field given by a function $e(t)$. We neglect here a possible dependence of $e(t)$ on the transverse position of the particle in the beam, as well as polarization effects, using a scalar quantity e. The exact mechanism of radiation does not matter here: it may be a synchrotron or undulator, or any other type of radiation. If the longitudinal position of the kth particle within the bunch is marked by a time variable t_k, the total radiated field $E(t)$ of all particles is

$$E(t) = \sum_{k=1}^{N} e(t-t_k), \quad (52)$$

where N is the number of particles in the bunch. We assume that t_k are random numbers, with the probability of finding t_k between t and $t+dt$ equal to $f(t)dt$, where $f(t)$ is the bunch distribution function [normalized so that $\int_{-\infty}^{\infty} f(t)dt = 1$]. For a Gaussian distribution, $f(t) = (2\pi\sigma_t^2)^{-1/2}e^{-t^2/2\sigma_t^2}$, where σ_t is the bunch length in units of time. We also assume that positions of different particles in the bunch, t_k and t_i for $k \neq i$, are uncorrelated, $\langle t_k t_i\rangle = \langle t_k\rangle\langle t_i\rangle$, with angular brackets denoting the averaging.

The spectral properties of the radiation are determined by the Fourier transform $\hat{E}(\omega)$ of the radiated field:

$$\hat{E}(\omega) = \hat{e}(\omega)\sum_{k=1}^{N} e^{i\omega t_k},$$

where $\hat{e}(\omega) = \int_{-\infty}^{\infty} e(t)e^{i\omega t}dt$. In the experiment, one is interested in the spectrum of the radiation $P(\omega)$, which is proportional to $|\hat{E}(\omega)|^2$ [we take $P(\omega) = |\hat{E}(\omega)|^2$ for brevity]:

$$P(\omega) = |\hat{e}(\omega)|^2\sum_{k,l=1}^{N} e^{i\omega(t_k-t_l)}. \quad (53)$$

Averaging this equation over all possible positions of an electron with the help of the distribution

function f, we find that

$$\langle P(\omega)\rangle = |\hat{e}(\omega)|^2 \sum_{k,l=1}^{N} \int_{-\infty}^{\infty}\int_{-\infty}^{\infty} dt_k dt_l \times f(t_k) f(t_l) e^{i\omega(t_k - t_l)} = |\hat{e}(\omega)|^2 (N + N^2 |\hat{f}(\omega)|^2), \quad (54)$$

where $\hat{f}(\omega) = \int_{-\infty}^{\infty} f(t) e^{i\omega t} dt$ is the Fourier transform of the distribution function [for the Gaussian distribution mentioned above, $\hat{f}(\omega) = e^{-\omega^2/2\sigma_t^2}$], and we approximated $N - 1 \approx N$. The first term of Eq. (54) is incoherent radiation proportional to the number of particles in the bunch. The second term is the coherent radiation that scales quadratically with N.

The coherent radiation term carries information about the distribution function of the beam but only at relatively low frequencies of the order of $\omega \lesssim \sigma_t^{-1}$, where $\hat{f}(\omega)$ is not negligible. At high frequencies, where $N|\hat{f}(\omega)|^2 \ll 1$, the coherent radiation is small in comparison with the incoherent radiation. However, the original, not averaged, expression for the spectral power (53) shows that the properties of the radiation even at high frequencies carry information about the distribution function. Indeed, each term, $e^{i\omega(t_k - t_l)}$, considered separately, oscillates as a function of frequency, with the period $\Delta\omega = 2\pi/(t_k - t_l) \sim 2\pi/\sigma_t$. Because of the random distribution of particles in the bunch, the sum in Eq. (53) fluctuates randomly as a function of frequency ω, and statistical properties of these fluctuations depend on the distribution function of the bunch.

To obtain a quantitative characteristic of these fluctuations, we first calculate the average value of the product $P(\omega)P(\omega')$:

$$\langle P(\omega)P(\omega')\rangle = |\hat{e}(\omega)|^2 |\hat{e}(\omega')|^2 \sum_{k,l,m,n=1}^{N} \times \langle e^{i\omega(t_k - t_l) + i\omega'(t_m - t_n)}\rangle.$$

Assuming that $N|f(\omega)|^2, N|f(\omega')|^2 \ll 1$ (which means that we can neglect the coherent radition at frequencies ω and ω'), it is straightforward to show that

$$\langle P(\omega)P(\omega')\rangle = N^2 |\hat{e}(\omega)|^2 |\hat{e}(\omega')|^2 \times (1 + |\hat{f}(\omega - \omega')|^2), \quad (55)$$

where the contribution to the final result comes from the terms with $k = l, m = n, k \neq m$ and $k = n, l = m, k \neq l$.

Let us now assume that the spectral measurement is performed with a narrow bandpass filter which is characterized by a transmission coefficient $T(\omega)$. The measured signal $\mathcal{E}$ is a fluctuating quantity,

$$\mathcal{E} = \int_{-\infty}^{\infty} P(\omega) T(\omega) d\omega, \quad (56)$$

with the average value $\langle\mathcal{E}\rangle = \int_{-\infty}^{\infty} \langle P(\omega)T(\omega)\rangle d\omega$. To calculate the fluctuation of the signal $\Delta\mathcal{E} = \mathcal{E} - \langle\mathcal{E}\rangle$, we will compute the quantity

$$\delta^2 = \frac{\langle \Delta\mathcal{E}^2\rangle}{\langle\mathcal{E}\rangle^2} = \langle\mathcal{E}\rangle^{-2} \int_{-\infty}^{\infty} TT' \langle [P - \langle P\rangle][P' - \langle P'\rangle]\rangle d\omega = \langle\mathcal{E}\rangle^{-2} \int_{-\infty}^{\infty} TT' [\langle PP'\rangle - \langle P\rangle\langle P'\rangle] d\omega, \quad (57)$$

where we have used the notation $P = P(\omega)$, $P' = P(\omega')$. We now use Eqs. (54) (where we neglect the N^2 term) and (55) for the average power $\langle P\rangle$ and the averaged product $\langle PP'\rangle$ to obtain

$$\delta^2 = \left(\int_{-\infty}^{\infty} T d\omega\right)^{-2} \int_{-\infty}^{\infty} TT' |\hat{f}_t(\omega - \omega')|^2 d\omega. \quad (58)$$

The integrals in Eq. (58) can be easily calculated if we assume a Gaussian profile for the function $T, T(\omega) = T_0 e^{-(\omega - \omega_0)^2/2\sigma_\omega^2}$, where ω_0 and σ_ω are respectively the central frequency of the filter, and where we have assumed that σ_ω is much smaller than the spectral width of the radiation. The result is

$$\delta^2 = \frac{1}{\sqrt{1 + 4\sigma_\omega^2 \sigma_t^2}}. \quad (59)$$

The expression (59) shows the potential of fluctuation analysis for measuring the absolute length of a bunch. If the frequency acceptance of the system, σ_ω, is known, then by measuring δ it is possible to derive the absolute value of the rms bunch length. For $\sigma_t \gg 1/2\sigma_\omega$, Eq. (59) becomes $\delta^2 \simeq 1/2\sigma_\omega\sigma_t$, and using the fact that the longitudinal coherence length of an electromagnetic mode with frequency content σ_ω is $\sigma_{tc} = 1/2\sigma_\omega$, we can write

$$\delta^2 \simeq \frac{\sigma_{tc}}{\sigma_t} = \frac{1}{M}, \quad (60)$$

where M is the number of modes contained in the bunch. Equation (60) leads to the physical

interpretation that the intensity fluctuation is due to M independent longitudinal modes radiating randomly within the bunch.

The theory outlined above was corroborated by several experiments. The reader can find details of these studies in the original publications [60–62]. In addition to measuring the rms bunch length, the method allows one to infer some information about the shape of the longitudinal distribution function of particles [62].

11. Fluctuations and Correlations

Averaging Eq. (53) over the distribution function to obtain (54) relied on the fact that particles' positions in the bunch are not correlated. Indeed, (53) involves terms that depend on positions of pairs of particles. Strictly speaking, it should be averaged with a *two-particle* distribution function $f_2(t_1, t_2)$, defined in such a way that $f_2(t_1, t_2)dt_1dt_2$ gives a probability of finding one of the particles within the interval dt_1 near point t_1 and at the same time finding the second particle within dt_2 near point t_2. In Eq. (54) we assumed that $f_2(t_1, t_2) = f(t_1)f(t_2)$, where $f(t)$ is a *one-particle* distribution. In case where there are such correlations, a more general expression for the distribution function reads (see e.g. Ref. 63)

$$f_2(t_1, t_2) = f(t_1)f(t_2) + g(t_1, t_2), \tag{61}$$

where $g(t_1, t_2)$ is the *correlation function*. Neglecting the second term on the right hand side of this equation is valid if there are no correlations in the beam. Taking account of g we obtain an additional contribution to (54) which we denote by $\langle P(\omega)_{\rm cor}\rangle$:

$$\langle P(\omega)_{\rm cor}\rangle = N^2|\hat{e}(\omega)|^2 \int_{-\infty}^{\infty}\int_{-\infty}^{\infty} dt_1dt_2g(t_1, t_2) \times e^{i\omega(t_1-t_2)}. \tag{62}$$

If we assume that $g(t_1, t_2) = G(t_1 - t_2)$ for $0 < t_1, t_2 < T_b$, where T_b is the bunch length in units of time, then

$$\begin{aligned}\langle P(\omega)_{\rm cor}\rangle &= N^2|\hat{e}(\omega)|^2 \int_{-\infty}^{\infty}\int_{-\infty}^{\infty} dt_1dt_2G(t_1 - t_2) \times e^{i\omega(t_1-t_2)} \\ &= N^2|\hat{e}(\omega)|^2\hat{G}(\omega),\end{aligned} \tag{63}$$

i.e. it is proportional to the Fourier transform of the correlation function. In Eq. (63) we assumed that T_b is much larger than the correlation time defined by the function G.

The above calculation illustrates the point that correlations between particles' positions in the beam can dramatically change statistical properties of radiation. This should not be surprising; a good example of such an effect is a self-amplified spontaneous emission free electron laser (SASE FEL). In such an FEL a specific beam instability leads to amplification of initial shot noise in the beam and establishes correlations between the particles. Detailed studies of statistical properties of FEL radiation can be found in the original papers [64–66].

12. Radiative Reaction Force and Coherent Radiation

When a bunch of relativistic particles emits radiation, the energy of the electromagnetic field is taken from the kinetic energy of the radiating particles. The energy balance in the process is maintained through a force that acts in the direction opposite to the velocity of the particles. This force is called the *radiative reaction force*.

One can find general expressions for the radiative reaction force in the case of a single radiating electron (point charge) in textbooks [17, 18]. In the limit of small nonrelativistic velocities, this force is proportional to the second derivative of the velocity with respect to time and, in addition to the expected damping effect, it exhibits a so-called "runaway" solution with exponentially growing acceleration on a timescale of the order of e^2/mc^3. This is sometimes considered as a serious deficiency of the force and a possible source of controversy, although a simple recipe for how to avoid the spurious solution is well known: one has to use the radiative reaction as a perturbation force for a regular motion of the particle [17].

For an ensemble of particles radiating coherently, one has to include in the consideration the effect of mutual interaction of particles in the process of radiation and the energy loss due to the interaction forces. In accelerator research the radiative reaction force is usually called the *CSR wakefield* or *CSR force*, with CSR standing for "coherent synchrotron radiation." An extensive review of the history of the subject can be found in Ref. 67.

There are two approaches to calculation of the CSR wake field. In the first approach one finds the electric field in the vicinity of a point charge moving along a given trajectory, and then adds contributions of all charges in the beam to obtain the radiative field at a given point inside the bunch. A systematic analysis based on this approach for a circular motion of a relativistic particle was carried out in Ref. 68 for the case of free space as well as the motion between two conducting plates parallel to the orbit plane. The total field of the point charge exhibits a singularity at the location of the charge, and one has to be careful to separate the singular Coulomb field from the radiative one. To uniquely identify the Coulomb term, it was proposed in Ref. 69 to subtract the field of the charge moving in the same direction along a straight line with constant velocity. Since such a charge does not radiate, there is only (relativistically transformed) Coulomb force in this case, which does not result in the energy loss of the beam, but leads to the energy exchange between different particles.

In a different approach, one can avoid problems associated with the subtraction of the singular Coulomb field by considering the beam as a charged medium with given densities of space charge and current, and using retarded potentials [Eqs. (7) and (8)] for direct calculation of the field. We will illustrate this approach below following the original paper [70].

We first note that the integrands in the expressions (8) have singularities when $\mathbf{r} \to \mathbf{r}'$; however, for a smooth distribution of charges in three-dimensional space these singularities are integrable, and the resulting potentials and fields are continuous functions of $\mathbf{r}$. This is not true, though, if one considers the beam as a line charge, neglecting its transverse size. It is remarkable, however, that the radiative reaction force remains finite even in this limit and can be easily calculated.

Let us consider a bunch that is moving along a circular trajectory of radius ρ. Denote the linear charge density of the line charge beam by $\lambda(s,t)$, where s is the arc length measured along the circular path of motion. Since we assume that each particle is moving with a constant velocity v, λ actually depends on the combination $\zeta = s - vt$. In addition, we will make the assumption that the electromagnetic fields on the orbit also depend only on the difference $\zeta = s - vt$; in other words, the field distribution on the orbit is transported together with the beam without changes. Physically, this assumption means that we neglect transient effects associated with injection of the beam to the circular orbit and assume that a steady state electromagnetic field has been established.

We are interested in the longitudinal electric field $E_\parallel = -\partial\phi/\partial s - \partial A_\parallel/\partial ct$, where $A_\parallel = \mathbf{A}\cdot\boldsymbol{\tau}$, with $\boldsymbol{\tau}$ the unit tangential vector to the orbit. This field is responsible for the energy change of the particles. Due to the fact that the functions ϕ and $A_\parallel$ depend on the difference $\zeta = s - vt$ only, we can also write

$$E_\parallel = -\frac{\partial(\phi - \beta A_\parallel)}{\partial s}. \tag{64}$$

Using (8) we find that

$$\phi - \beta A_\parallel = \int ds'\lambda(s', t_{\rm ret})\frac{1 - \beta^2\boldsymbol{\tau}(s)\cdot\boldsymbol{\tau}(s')}{|\mathbf{r}(s) - \mathbf{r}(s')|}, \tag{65}$$

where $\boldsymbol{\tau}(s)$ is the tangential vector in the direction of motion at point s, $|\mathbf{r}(s) - \mathbf{r}(s')|$ is the distance between the points s and s', and $t_{\rm ret}(s, s', t) = t - |\mathbf{r}(s) - \mathbf{r}(s')|/c$.

First, we note that this integral diverges if $\beta \neq 1$. This is due to the fact that the space charge effects are infinitely large for a line charge beam. This difficulty can be avoided if we take the limit $\gamma \to \infty$ and set $\beta = 1$. We then assume that only a small part of the circle contributes to the integral, and use Taylor expansion assuming that $|s - s'| \ll \rho$. One can show that the main contribution to the integral in the ultrarelativistic limit comes from the region $s' < s$, i.e. only preceding points of the orbit contribute to s. A simple geometrical consideration then gives $|\mathbf{r}(s) - \mathbf{r}(s')| \approx (s - s') - (s - s')^3/24\rho^2$ and $1 - \boldsymbol{\tau}(s)\cdot\boldsymbol{\tau}(s') \approx (s - s')^2/2\rho^2$. We also take into account that $\lambda(s', t_{\rm ret})$ actually depends on the difference of the arguments, $\lambda(s' - ct_{\rm ret})$. Equation (65) can now be written as

$$\begin{aligned}
\phi - \beta A_\parallel &= \int_{-\infty}^{s} ds'\lambda(s' - ct_{\rm ret})\frac{1}{2\rho^2}(s - s') \\
&= \int_{-\infty}^{s} ds'\lambda(s - ct - (s - s')^3/24\rho^2) \\
&\quad\times \frac{1}{2\rho^2}(s - s') \\
&= \frac{1}{2\rho^2}\frac{1}{3}(24\rho^2)^{1/3} \\
&\quad\times \int_0^\infty ds'\lambda(s - ct - \xi)\xi^{-1/3},
\end{aligned} \tag{66}$$

where the new integration variable is $\xi = (s - s')^3/24\rho^2$. Finally, using (64) we find the electric field in the beam

$$E_\parallel = -\frac{2}{\rho^{2/3}3^{1/3}}\int_0^\infty ds'\lambda'(s-ct-\xi)\xi^{-1/3}, \tag{67}$$

where λ' is the derivative of λ with respect to its argument. Analysis shows that typically this field accelerates particles in the head of the bunch, and decelerates in the tail, with the total deceleration prevailing. Moreover, it can be proven that the energy loss due to the field $E_\parallel$ is exactly equal to the coherent radiation power of the beam [69], as was mentioned at the beginning of this section.

The result derived in this section represents one of the simplest problems in the theory of the CSR wake field. The reader can find further development of the concept, as well as its application to practical accelerator research, in the original publications [47, 71–77].

Appendix

To derive Eq. (15) we use the Liénard–Wiechert potentials (10) and the first equation in (7). We first make the Fourier transformation of Eq. (7):

$$\hat{\mathbf{E}}(\mathbf{r},\omega) = \int_{-\infty}^{\infty}\left(\frac{i\omega}{c}\hat{\mathbf{A}} - \nabla\hat{\phi}\right)e^{i\omega t}dt. \tag{A.1}$$

Using the retarded time t' as a new integration variable instead of t, with $dt = (1 - \mathbf{n}\cdot\boldsymbol{\beta})dt'$, we find that

$$\begin{aligned}\hat{\mathbf{E}}(\mathbf{r},\omega) &= \frac{ie\omega}{c}\int_{-\infty}^{\infty}dt'\frac{\boldsymbol{\beta}}{R}e^{i\omega(t'+R/c)} \\ &\quad - e\nabla\int_{-\infty}^{\infty}dt'\frac{1}{R}e^{i\omega(t'+R/c)} \\ &= \frac{ie\omega}{c}\int_{-\infty}^{\infty}dt'\frac{\boldsymbol{\beta}}{R}e^{i\omega(t'+R/c)} \\ &\quad + e\int_{-\infty}^{\infty}dt'\mathbf{n}\left(\frac{1}{R^2} - \frac{i\omega}{Rc}\right)e^{i\omega(t'+R/c)} \\ &= \frac{ie\omega}{c}\int_{-\infty}^{\infty}\frac{dt'}{R}\left[\boldsymbol{\beta} - \mathbf{n}\left(1 + \frac{ic}{\omega R}\right)\right] \\ &\quad \times e^{i\omega(t'+R/c)}.\end{aligned}$$

Replacing the dummy integration variable t' with t, this equation gives Eq. (15).

References

[1] G. Schott, *Electromagnetic Radiation* (Cambridge, 1912).
[2] J. Schwinger (1945), unpublished.
[3] M. Furman (ed.), Rep. LBL-39088 (1996).
[4] J. Schwinger, *Phys. Rev.* **75**, 1912 (1949).
[5] L. Schiff, *Rev. Sci. Instrum.* **17**, 6 (1946).
[6] J. S. Nodvick and D. S. Saxon, *Phys. Rev.* **96**, 180 (1954).
[7] K. Kurokawa, *An Introduction to the Theory of Microwave Circuits* (Academic, New York, 1969).
[8] L. A. Vainshtein, *Electromagnetic Waves* (Radio i svyaz', Moscow, 1988), in Russian.
[9] R. E. Collin, *Field Theory of Guided Waves*, 2nd edn. (IEEE Press, New York, 1991).
[10] M. Sands, *Tech. Rep.* SLAC-121, (SLAC, 1970).
[11] A. A. Sokolov and I. M. Ternov, *Sov. Phys. Dokl.* **8**, 1203 (1964).
[12] C. B. Schroeder, C. Pellegrini and P. Chen, *Phys. Rev. E* **64**, 056502 (2001).
[13] F. Reitich and K. K. Tamma, *Comput. Methods Eng. Sci.* **5**, 287 (2004).
[14] A. Bondeson, T. Rylander and P. Ingelström, *Computational Electromagnetics* (Springer, 2005).
[15] A. F. Peterson, S. L. Ray and R. Mittra, *Computational Methods for Electromagnetics* (IEEE Press, 1998).
[16] A. F. Peterson, S. L. Ray and R. Mittra, *Numerical Methods in Computational Electrodynamics: Linear Systems in Practical Applications* (Springer, 2001).
[17] L. D. Landau and E. M. Lifshitz, *The Classical Theory of Fields*, Vol. 2 of *Course of Theoretical Physics* 4th edn. (Pergamon, London, 1979) (transl. from the Russian).
[18] J. D. Jackson, *Classical Electrodynamics*, 3rd edn. (Wiley, New York, 1999).
[19] L. D. Landau and E. M. Lifshitz, *Electrodynamics of Continuous Media*, Vol. 8 of *Course of Theoretical Physics* (Pergamon, London, 1960), 2nd edn. (translated from the Russian).
[20] J. D. Jackson, *Am. J. Phys.* **70**, 917 (2002).
[21] K.-J. Kim, in *Physics of Particle Accelerators* (AIP, New York, 1989), AIP Conf. Proc. No. 367, pp. 565–632.
[22] A. Hofmann, *The Physics of Synchrotron Radiation* (Cambridge University Press, 2004).
[23] H. Wiedemann, *Particle Accelerator Physics II* (Springer-Verlag, Berlin, 1999).
[24] A. Hofmann, *Reviews of Accelerator Science and Technology*, Vol. 1 (World Scientific, 2008), p. 121.

[25] R. A. Bosch, *Il Nuovo Cimento D* **20**, 483 (1998).
[26] O. V. Chubar, *Rev. Sci. Instrum.* **66**(2), 1872 (1995).
[27] O. Chubar and P. Elleaume, in *Proc. 6th European Particle Accelerator Conference* (1998), p. 1177.
[28] G. Geloni, E. L. Saldin, E. A. Schneidmiller and M. V. Yurkov, *Nucl. Instrum. Methods Phys. Res. A* **528**, 326 (2004).
[29] G. Stupakov, *Lecture Notes on Classical Mechanics and Electromagnetism in Accelerator Physics* (The US Particle Accelerator School, Albuquerque, NM, 2009).
[30] K.-J. Kim, K. T. McDonald, G. V. Stupakov and M. S. Zolotorev, *Phys. Rev. Lett.* **84**, 3210 (2000).
[31] G. Geloni, E. Saldin, E. Schneidmiller and M. Yurkov, Rep. 03-031 (DESY, 2003).
[32] R. A. Bosch, T. E. May, R. Reininger and M. A. Green, *Rev. Sci. Instrum.* **67**, 1 (1996).
[33] V. G. Bagrov, N. I. Fedosov and I. M. Ternov, *Phys. Rev. D* **28**, 2464 (1983).
[34] M. L. Ter-Mikaelian, *High-Energy Electromagnetic Processes in Condensed Media* (Wiley-Interscience, New York, 1972).
[35] V. B. Berestetskii, E. M. Lifshitz and L. P. Pitaevskii, *Quantum Electrodynamics*, Vol. 4 of *Course of Theoretical Physics* (Pergamon, London, 1982), 2nd edn. (transl. from the Russian).
[36] R. L. Warnock and P. Morton, *Part. Accel.* **25**, 113 (1990).
[37] K.-Y. Ng, *Part. Accel.* **25**, 153 (1990).
[38] M. Lentovich and V. Fock, *J. Phys. USSR* **10**, 13 (1946).
[39] B. Saleh and M. Teich, *Fundamentals of Photonics*, 2nd edn. (Wiley-Interscience, 2007)
[40] E. L. Saldin, E. A. Schneidmiller and M. V. Yurkov, *The Physics of Free Electron Lasers* (Springer, 2000).
[41] G. Geloni, E. Saldin, E. Schneidmiller and M. Yurkov, Rep. 05-032 (DESY, 2005).
[42] G. Stupakov, *New J. Phys.* **8**, 280 (2006).
[43] G. Stupakov, preprint SLAC-PUB-13661, (SLAC, 2009).
[44] I. Zagorodnov and T. Weiland, *Phys. Rev. ST Accel. Beams* **8**, 042001 (2005).
[45] G. V. Stupakov and I. A. Kotelnikov, *Phys. Rev. ST Accel. Beams* **6**, 034401 (2003).
[46] T. Agoh and K. Yokoya, *Phys. Rev. ST Accel. Beams* **7**, 054403 (2004).
[47] G. Stupakov and I. A. Kotelnikov, *Phys. Rev. ST Accel. Beams* **12**, 104401 (2009).
[48] T. Agoh, *Phys. Rev. ST Accel. Beams* **12**, 094402 (2009).
[49] G. Dome, E. Gianfelice, L. Palumbo, V. G. Vaccaro and L. Verolino, *Nuovo Cimento A* **104**, 1241 (1991).
[50] B. M. Bolotovskii and E. A. Galst'yan, *Phys. Usp.* **43**, 755 (2000).
[51] I. Gradshteyn and I. Ryzhik, *Table of Integrals, Series, and Products*, 6th edn. (Academic, 2000).
[52] B. M. Bolotovskii and E. A. Galstyan, *Phys. Usp.* **43**, 755 (2000), http://ufn.ru/en/articles/2000/8/a
[53] Z. Huang, G. Stupakov and M. Zolotorev, *Phys. Rev. ST Accel. Beams* **7**, 011302 (2004).
[54] P. Karataev, S. Araki, A. Aryshev, G. Naumenko, A. Potylitsyn, N. Terunuma and J. Urakawa, *Phys. Rev. ST Accel. Beams* **11**, 032804 (2008).
[55] D. Xiang, W.-H. Huang, Y.-Z. Lin, S.-J. Park and I. S. Ko, *Phys. Rev. ST Accel. Beams* **11**, 024001 (2008).
[56] D. Xiang, W.-H. Huang and Y.-Z. Lin, *Phys. Rev. ST Accel. Beams* **10**, 062801 (2007).
[57] R. B. Fiorito, A. G. Shkvarunets, T. Watanabe, V. Yakimenko and D. Snyder, *Phys. Rev. ST Accel. Beams* **9**, 052802 (2006).
[58] M. Zolotorev and G. Stupakov, preprint SLAC-PUB-7132 (SLAC, 1996).
[59] J. Krzywinski, E. L. Saldin, E. A. Schneidmiller and M. V. Yurkov, *Nucl. Instrum. Methods, Sec. A* **401**, 429 (1997).
[60] F. Sannibale, G. V. Stupakov, M. S. Zolotorev, D. Filippetto and L. Jägerhofer, *Phys. Rev. ST Accel. Beams* **12**, 032801 (2009).
[61] P. Catravas, W. P. Leemans, J. S. Wurtele, M. S. Zolotorev, M. Babzien, I. Ben-Zvi, Z. Segalov, X.-J. Wang and V. Yakimenko, *Phys. Rev. Lett.* **82**, 5261 (1999).
[62] V. Sajaev, in *Proc. European Particle Accelerator Conference* (Vienna, 2000), p. 1806.
[63] R. Balescu, *Equilibrium and Nonequilibrium Statistical Mechanics* (Wiley-Interscience, New York, 1975).
[64] E. L. Saldin, E. A. Schneidmiller and M. V. Yurkov, *Opt. Commun.* **148**, 383 (1998).
[65] S. Krinsky and Y. Li, *Phys. Rev. E* **73**, 066501 (2006).
[66] E. L. Saldin, E. A. Schneidmiller and M. V. Yurkov, *New J. Phys.* **12**, 035010 (2009).
[67] J. B. Murphy, *Beam Dyn. Newslett.* **35**, 21 (2004).
[68] J. B. Murphy, S. Krinsky and R. L. Gluckstern, *Part. Accel.* **57**, 9 (1997).
[69] E. L. Saldin, E. A. Schneidmiller and M. V. Yurkov, *Nucl. Instrum. Methods A* **398**, 373 (1997).
[70] Y. S. Derbenev, J. Rossbach, E. L. Saldin and V. D. Shiltsev, DESY FEL Rep. TESLA-FEL 95-05 (Deutsches Elektronen-Synchrotron, Hamburg, 1995).
[71] E. L. Saldin, E. A. Schneidmiller and M. V. Yurkov, *Opt. Commun.* **148**, 383 (1998).
[72] G. Stupakov and P. Emma, in *Proc. 8th European Particle Accelerator Conference* (Paris, 2002), p. 1479.
[73] J. Wu, T. Raubenheimer and G. Stupakov, *Phys. Rev. ST Accel. Beams* **6**, 040701 (2003).

[74] R. Talman, *Phys. Rev. ST Accel. Beams* **7**, 100701 (2004).
[75] R. Warnock, G. Bassi and J. Ellison, *Nucl. Instrum. Methods Phys. Res. Sec. A:* **558**, 85 (2006); *Proc. 8th International Computational Accelerator Physics Conference* (ICAP 2004).
[76] R. Li, *Phys. Rev. ST Accel. Beams* **11**, 024401 (2008).
[77] C. Mayes and G. Hoffstaetter, *Phys. Rev. ST Accel. Beams* **12**, 024401 (2009).

Gennady Stupakov is Collective Effects Group leader at the SLAC National Accelerator Laboratory. He started his scientific career as a plasma physicist at the Budker Institute in Novosibirsk, Russia. He had moved to the US in 1991 and switched to accelerator physics, working at the Superconducting Supercollider in Dallas, Texas. After the shutdown of the SSC, he joined SLAC, continuing research on various aspects of collective effects of the beams of charged particles. His current interests involve the FEL theory, coherent synchrotron radiation instability, laser acceleration in vacuum, and various aspects of the wake field calculations in accelerators. He is a Fellow of the American Physical Society.